Eur. Phys. J. D (2020) 74: 46
https://doi.org/10.1140/epjd/e2020-100639-y

THE EUROPEAN PHYSICAL JOURNAL D

Regular Article

Electron scattering from allene and 1,2-butadiene*

Giseli M. Moreira[1], Thiago C. Freitas[2], and Márcio H. F. Bettega[1,a]

[1] Departamento de Física, Universidade Federal do Paraná, Caixa Postal 19044, 81531-980 Curitiba, Paraná, Brazil
[2] Setor de Educação Profissional e Tecnológica, Universidade Federal do Paraná, R. Dr. Alcides Vieira Arcoverde, 1225, 81520-260 Curitiba, Paraná, Brazil

Received 19 December 2019 / Received in final form 27 January 2020
Published online 12 March 2020

Abstract. The Schwinger multichannel method is employed to calculate elastic cross sections for electron collisions with allene (C_3H_4) and 1,2-butadiene (C_4H_6) molecules. Integral elastic and differential cross sections were obtained for both molecules in the static-exchange and static-exchange-polarization approximations, for energies from 0.1 eV to 10 eV. Both molecules have a π^* shape resonance centered at 2.4 eV in the integral cross section, and a Ramsauer-Townsend minimum was found at around 0.34 eV in the allene cross section. The present differential elastic cross sections are compared between the two molecules and with the experimental and theoretical data available. Some of the features in the cross sections are analyzed and discussed in the context of the methylation effect, since the 1,2-butadiene molecule can be viewed as the methylated allene molecule. Electronic structure calculations are also performed in order to help in the interpretations of our results.

1 Introduction

Hydrocarbons are abundant compounds in nature, playing important roles in a wide range of phenomena, like fuel combustion [1], interstellar clouds, as pointed by Szmytkowski and Kwitneski [2], planetary atmospheres [3], and plasma technology [4–6]. Despite all these fields with fundamental and practical interest, the data for some processes related to hydrocarbons still remain sparse and fragmentary. When one of the H atoms of the allene molecule is replaced by a CH_3 group, we obtain the 1,2-butadiene molecule through a methylation process. Besides our interest in the methylation effect in electron-molecule collisions, the present study also focuses on providing theoretical data for electron collisions with allene and 1,2-butadiene, where for the latter the results are scarce.

Earlier studies on electron interactions with 1,2-butadiene by Collin and Lossing [7] focused only in the energetic of ionization and positive ion formation. The first measurement of the total cross section (TCS) for electron scattering by 1,2-butadiene was performed by Szmytkowski et al. [9], employing the linear electron-beam transmission, for the energy range from 0.5 eV to 300 eV. They have found a sharp structure located at around 2.3 eV, which is probably related to a shape resonance associated with the vacant π^* orbital of the C=C bond. A broad structure between 5 eV and 14 eV was also reported, but it was not precisely assigned to a particular state of the molecule.

A linear electron-beam transmission experiment was employed by Szmytkowski and Kwitnewski [2] to measure the absolute total cross section for electron collisions with allene and other molecules, for the energy range from 0.5 eV to 370 eV. A peak centered at 2.3 eV was reported in the TCS, and associated with the formation of a shape-resonance. A shoulder near 6 eV and a structure centered at 14 eV were also reported. Absolute differential cross sections (DCS) for electron collisions with C_3H_4 isomers, including allene, were measured by Nakano et al. [10] using the crossed beam technique from the energy of the incident electron between 1.5 eV and 100 eV. A resonance centered at 2.9 eV was reported together with peaks centered at around 12 eV and 14 eV, also pointed by the authors as being resonances. Makochekanwa et al. [11] measured TCS for electron (and also positron) collisions with allene and propyne using the linear transmission method with the energy ranging from 0.8 eV to 600 eV. They have also obtained the elastic cross section, in a crossed beam experiment, for electron scattering by the same molecules in the energy range from 2 eV until 100 eV. For allene, it has been reported sharp structures at around 2.5 eV and 11 eV. The first one associated with a π^* shape resonance and the second one with a set of combined partial waves.

* Contribution to the Topical Issue "Low-Energy Positron and Positronium Physics and Electron-Molecule Collisions and Swarms (POSMOL 2019)", edited by Michael Brunger, David Cassidy, Sača Dujko, Dragana Maric, Joan Marler, James Sullivan, Juraj Fedor.

[a] e-mail: bettega@fisica.ufpr.br

The Schwinger multichannel method was previously employed to compute elastic integral, differential cross-sections and rotational excitation cross sections of allene and of other C_3H_4 isomers [12,13]. Total and differential cross sections were computed for a wide energy range by Barot et al. [14]. The authors used the R-matrix method for energies below 10 eV and the spherical complex optical potential formalism for higher energies, ranging from 10 eV to 2000 eV. They reported a π^* shape resonance located at around 2.9 eV.

In this paper we report elastic integral and differential cross sections for electron scattering by allene and 1,2-butadiene molecules. Since 1,2-butadiene can be considered as a methylated allene, we also investigate the methylation effect in the cross sections of these two targets. The remainder of this paper is organized as follows. In Section 2 we briefly present the main aspects of the theory employed to perform the calculations. Section 3 shows the present results in comparison with the available theoretical and experimental data followed by the analysis of our results. We conclude the paper in Section 4 with a summary of our findings.

2 Theory

The Schwinger Multichannel (SMC) method [15,16] and its implementations have been recently reviewed [17] and here we briefly describe those aspects that are important to the present calculations. The SMC method is a variational approach to the scattering amplitude which results in the following working expression

$$f^{\mathrm{SMC}}(\boldsymbol{k}_f, \boldsymbol{k}_i) = -\frac{1}{2\pi} \sum_{m,n} \langle S_{\boldsymbol{k}_f} | V | \chi_m \rangle \left(d^{-1}\right)_{mn} \langle \chi_n | V | S_{\boldsymbol{k}_i} \rangle, \tag{1}$$

where

$$d_{mn} = \langle \chi_m | A^{(+)} | \chi_n \rangle \tag{2}$$

and

$$A^{(+)} = \frac{1}{2}(PV + VP) - VG_P^{(+)}V + \frac{\hat{H}}{N+1} - \frac{1}{2}\left(\hat{H}P + P\hat{H}\right). \tag{3}$$

In the expressions above, $\{|\chi_m\rangle\}$ represent the $(N+1)$-electron trial configuration-state functions (CSF), which are products of target states with single-particle scattering orbitals with the proper spin-coupling. $|S_{\boldsymbol{k}_{i(f)}}\rangle$ is an eigenstate of the unperturbed Hamiltonian H_0, given by the product of a target state and a plane wave with momentum $\boldsymbol{k}_{i(f)}$ representing the free electron; V is the interaction potential between the incident electron and the target; $\hat{H} \equiv E - H$, where E is the collision energy and $H = H_0 + V$ is the scattering Hamiltonian; P is a projection operator onto the open-channel target space defined as

$$P = \sum_{l=1}^{\text{open}} |\Phi_l\rangle\langle\Phi_l|, \tag{4}$$

and $G_P^{(+)}$ is the free-particle Green's function projected on the P-space.

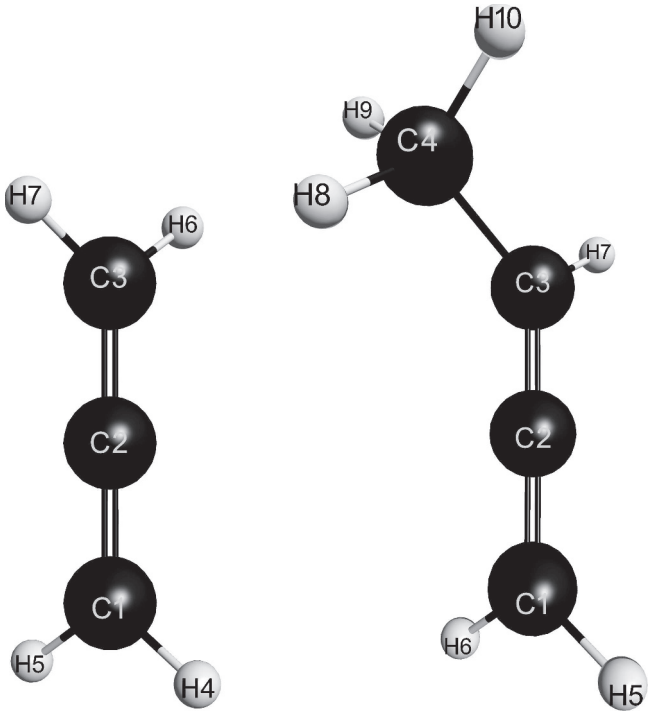

Fig. 1. Geometrical structures of allene (C_3H_4) on the left, and 1,2-butadiene (C_4H_6) on the right. The 1,2-butadiene molecule can be seen as allene molecule with a $-CH_3$ group replacing an H atom, the methylation. These structures were generated with MacMolPlt [21].

We considered the static-exchange (SE) and static-exchange plus polarization (SEP) approximations in our calculations. In the SE approximation, the $(N+1)$-electron basis set is constructed as

$$|\chi_m\rangle = \mathcal{A}|\Phi_1\rangle \otimes |\varphi_m\rangle \tag{5}$$

where $|\Phi_1\rangle$ is the Hartree–Fock target ground state, $|\varphi_m\rangle$ is a single-particle function which represents the continuum electron and $\mathcal{A}$ is the antisymmetrization operator. In the SEP approximation, the SE set is augmented by including configuration state functions constructed as

$$|\chi_{mn}\rangle = \mathcal{A}|\Phi_m\rangle \otimes |\varphi_n\rangle \tag{6}$$

where $|\Phi_m\rangle$ are N-electron Slater determinants obtained by performing single (virtual) excitations of the target. $|\varphi_n\rangle$ is also an single-particle function which represents the continuum electron and $\mathcal{A}$ is the antisymmetrizer.

Our calculations were carried out at the ground state optimized geometry obtained at the second order Møller–Plesset perturbation theory level with a 6-31G(1d) basis set using the computational package GAMESS [18]. The geometrical structures of allene and 1,2-butadiene molecules are shown in Figure 1, and the main geometrical parameters are tabulated and compared with experimental data in Table 1. The allene molecule belongs to the D_{2d} point group but the calculations were performed in the C_{2v} group, while the 1,2-butadiene molecule has C_s symmetry. We have employed the local-density *norm-conserving*

Table 1. Main geometrical parameters employed in the present calculations, with bond lengths (r) in angstroms and angles (a) are in degrees. Experimental values of these parameters for allene [19], and 1,2-butadiene [20] are show between parentheses when available.

C_3H_4	Value	C_4H_6	Value
rC1C2	1.3128 (1.308)	rC1C2	1.3138 (1.314)
rC1H4	1.0859 (1.087)	rC2C3	1.3144 (1.301)
aH4C2H5	117.2 (118.2)	rC3C4	1.5062 (1.515)
aH5C2C1	121.4 (120.9)	rC3H7	1.0900
		rC4H8	1.0948
		aC1C2C3	179.6 (179.5)
		aC2C3C4	124.1 (124.0)
		aH5C1C2	121.5
		aH7C3C2	118.6
		aH8C4C3	110.7
		aH9C4H8	108.5
		aH9C4H10	107.5

Table 2. Exponents of the Cartesian Gaussian functions used to represent the single-particle basis. For C atoms the functions are uncontracted, the contraction coefficients are for the H functions.

Type	Carbon	Hydrogen	Coefficient
s	12.49628	13.3615	0.130844
s	2.470286	2.0133	0.921539
s	0.614028	0.4538	1.0
s	0.184028	0.1233	1.0
s	0.039982		
p	5.228869	0.7500	1.0
p	1.592058		
p	0.568612		
p	0.210326		
p	0.072250		
d	1.794795		
d	0.420257		
d	0.101114		

pseudopotentials of Bachelet, Hamann and Schlüter [22] to represent the nuclei and the core electrons of the carbon atoms. The Cartesian Gaussian functions (single-particle basis) used for the carbon atoms included $5s5p3d$ functions, which are tabulated in Table 2 and were generated using a variational method described according to reference [23].

The polarization effects were included using improved virtual orbitals (IVOs) [24] to represent the particle and scattering orbitals (see Eq. (6)). For the allene molecule, we employed the 8 (valence) occupied orbitals as hole orbitals. The configuration space for the A_1 and A_2 symmetries was constructed using the first 52 IVOs with lowest eigenvalues as particle and scattering orbitals, and singlet- and triplet-coupled excitations, resulting in 6198 CSFs and 4695 CSFs, respectively. For the resonant B_1 and B_2 symmetries, we have performed calculations considering only the resonant b_1 and b_2 IVOs as scattering orbitals [25], and allowing only singlet-coupled excitations from the hole orbital and particle orbitals belonging to the same symmetry, resulting in 368 CSFs for each symmetry. The use of the lowest 52 IVOs as particle and scattering orbitals was also the criterion for the construction of the CSFs for 1,2-butadiene. As hole orbitals, we use the 11 (valence) occupied orbitals and thus resulting in 7891 CSFs for the A' symmetry, and 7444 CSFs for the A'', considering for both symmetries the singlet- and triplet-coupled excitations.

One of the results of the methylation effect is the permanent electric dipole moment in the 1,2-butadiene molecule, whose calculated and experimental values are 0.49 D and 0.40 D [26], respectively. In order to properly describe the long-range effects on the cross sections we employed the Born-closure procedure, as previously described in reference [27]. In this procedure, the low partial wave contributions are retained until a certain $\ell_{\max}$ value and the higher partial wave contributions are obtained in the first Born approximation for a point dipole moment with the same magnitude and orientation as the molecular dipole. The divergence's scattering amplitude in the frontal scattering is avoided using an approximation that takes into account the inelastic dipole-allowed rotational transitions (00 → 10 rotational excitation of an asymmetric top) [28], by making $k_f^2 = k_i^2 + 2\Delta E_{\rm rot}$ where $\Delta E_{\rm rot} = 1.59 \times 10^{-5}$ eV. For SE and SEP calculations, the values of $\ell_{\max}$ are summarized as $\ell_{\max} = 1$ for 0.1–0.4 eV; $\ell_{\max} = 2$ for 0.5–0.6 eV; $\ell_{\max}$=3 for 0.7–1.2 eV; $\ell_{\max} = 4$ for 1.3–2.5 eV; $\ell_{\max} = 5$ for 2.6 eV to 2.9 eV; $\ell_{\max} = 6$ for 3–8 eV; and $\ell_{\max} = 7$ for 8.1–10 eV.

3 Results and discussion

In Figure 2 we show the integral elastic cross section for electron collisions with allene in the SE and SEP approximations for energies from 0.1 eV to 10 eV. The SE cross section displays a broad resonance centered at 4.2 eV, while in the SEP results this structure moves down in energy to at around 2.4 eV. TCS obtained experimentally by Szmytkowski et al. [2], also shown in this figure, displays a low-energy structure located at 2.3 eV. Makochenkanwa et al. [11] also measured the TCS and found a resonant structure located at 2.5 eV. R-matrix TCS calculations by Barot et al. [14] located this structure at 2.9 eV, being higher than the experimental value. The calculations of Sanchez et al. [12] put the resonance's peak at 3 eV, also higher than the experiment. The structures that appear from 4 eV on the curve referring to the SEP calculation are called pseudoresonances, which come from channels that have energy to be open but are treated as closed channels. The threshold of the first excited state is 3.78 eV in Full Single CI calculation at the present optimized geometry and with the scattering basis set, and at 3.03 eV according to reference [8], while the present computed vertical ionization potential is 10.3 eV which compares well with the experimental value of 10.2 eV [26]. The excited electronic channels, and the vibrational and rotational channels which are not taken in to account in present in the integral

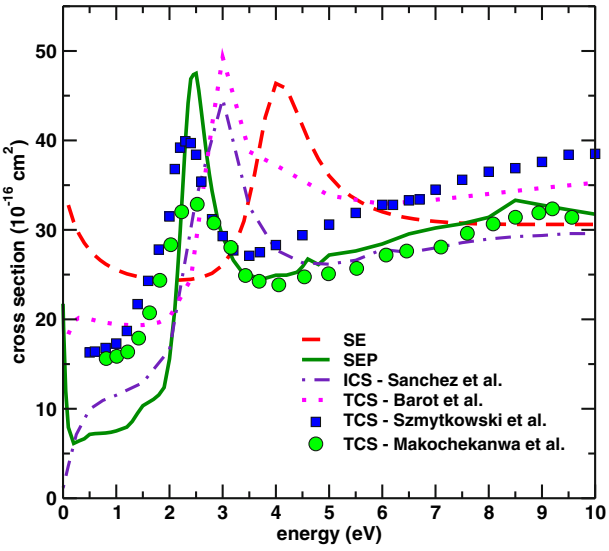

Fig. 2. Integral elastic cross section for electron collisions with allene in the SE and SEP approximations. Total cross sections measured by Szmytkowski et al. [2], Makochekanwa et al. [11], and calculated by Barot et al. [14] are also shown for comparison purposes. See text for discussion.

Table 3. Integral elastic cross sections (ICS) in the SEP approximation for electron impact on allene (C_3H_4) in units of 10^{-16} cm^2, energy (E) values are in units of eV.

E	ICS	E	ICS	E	ICS	E	ICS
0.1	7.9	1.7	11.0	2.70	38.4	4.3	25.0
0.2	6.1	1.8	11.5	2.75	36.2	4.4	25.3
0.3	6.4	1.9	12.4	2.80	34.3	4.5	25.9
0.4	6.6	2.0	15.6	2.90	31.4	4.6	26.7
0.5	7.1	2.1	21.1	2.95	30.2	4.7	26.4
0.6	7.2	2.15	25.1	3.0	29.2	4.8	26.1
0.7	7.2	2.20	29.7	3.1	27.7	5.5	27.6
0.8	7.3	2.25	34.8	3.2	26.6	6.0	28.4
0.9	7.4	2.30	39.9	3.3	26.1	6.5	29.5
1.0	7.2	2.35	44.2	3.4	25.0	7.0	30.2
1.1	7.7	2.40	46.9	3.5	25.0	7.5	30.7
1.2	7.9	2.45	47.4	3.6	24.7	8.0	31.4
1.3	8.6	2.50	47.5	3.7	24.7	8.5	33.3
1.4	9.5	2.55	45.6	3.8	24.6	9.0	32.8
1.5	10.3	2.60	43.2	4.0	24.9	9.5	32.2
1.6	10.9	2.65	40.7	4.2	24.9	10.0	31.7

cross section contribute to the difference in magnitude between our elastic cross section and the total cross sections.

According to Barot et al. [14] the correct positioning of the resonance and the cross section behavior in the low-energy range are intrinsically connected with the proper inclusion of electron correlations in the target and scattering wave functions. This is probably the cause of the energy difference between their resonance's position in comparison with the experiments. Previous SMC calculations by Sanchez et al. [12] did not find good agreement with experiment regarding the resonance energy probably due to the lack of polarization associated with the computational limitations at that time. The present SEP cross sections, tabulated in Table 3, are in good agreement with both experimental TCSs regarding the resonance's location, being more accurate than the previous calculations available in the literature, due to the improvement in the inclusion of polarization-correlation effects.

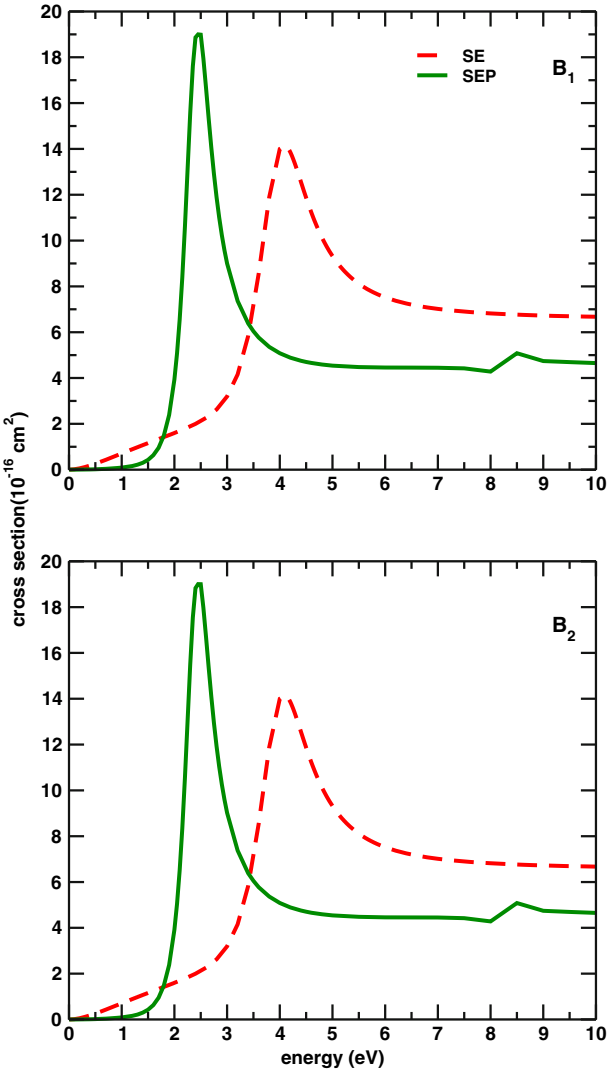

Fig. 3. Symmetry decomposition of the two resonant symmetries, in the C_{2v} point group, of the integral elastic cross section for electron collisions with allene in the SE and SEP approximations. See text for discussion.

In Figure 3 we show the symmetry decomposition of the integral cross section for allene, in the SE and SEP approximations. As already mentioned, our calculations were performed within the C_{2v} point group. This group presents four irreducible representations, but we will only show the cross section for the two resonant symmetries, B_1 and B_2. We see that these two symmetries are degenerated (they correspond to the two components of the E symmetry of D_{2d}), with the same contribution to the integral cross section, and with the structures at the very

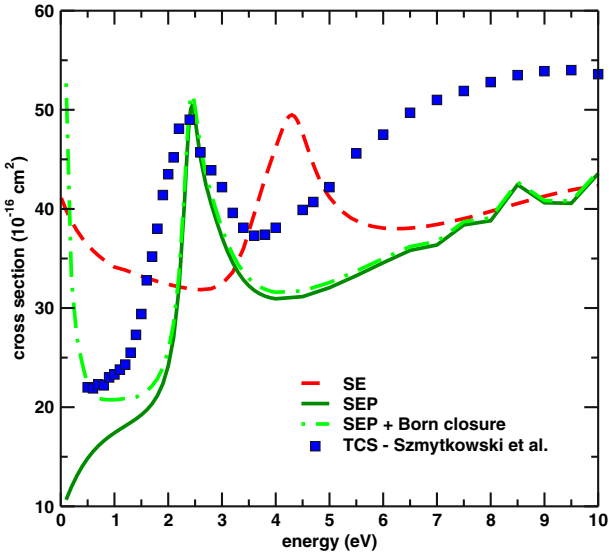

Fig. 4. Integral elastic cross section for electron collisions with 1,2-butadiene in the SE, SEP, and SEP with Born closure approximations. Total cross section measured by Szmytkowski et al. [2] is also shown for comparison purposes. See text for discussion.

Table 4. Integral elastic cross sections (ICS), in the SEP with Born closure approximation, for electron impact on 1,2-butdiene (C_4H_6) in units of 10^{-16} cm^2, energy (E) values are in units of eV.

E	ICS	E	ICS	E	ICS	E	ICS
0.1	52.7	1.6	21.6	2.46	51.4	3.8	31.9
0.2	32.9	1.7	22.1	2.48	50.9	3.9	31.7
0.3	26.0	1.8	22.9	2.5	50.2	4.0	31.6
0.4	24.4	1.9	24.0	2.6	46.2	4.5	31.7
0.5	22.2	2.0	25.7	2.7	43.5	5.0	32.6
0.6	21.7	2.1	28.5	2.8	41.5	5.5	33.7
0.7	20.9	2.2	33.3	2.9	39.7	6.0	35.0
0.8	20.8	2.3	41.7	3.0	38.0	6.5	36.2
0.9	20.7	2.32	43.7	3.1	36.6	7.0	36.7
1.0	20.8	2.34	45.8	3.2	35.4	7.5	38.7
1.1	20.8	2.36	47.7	3.3	34.4	8.0	39.1
1.2	20.9	2.38	49.3	3.4	33.6	8.5	42.7
1.3	20.8	2.4	50.5	3.5	33.0	9.0	40.8
1.4	21.0	2.42	51.3	3.6	32.5	9.5	40.8
1.5	21.3	2.44	51.6	3.7	32.2	10	43.8

same energy. In the SE results, the structure is located at around 4.2 eV, while in the SEP approximation this structure is now located at around 2.4 eV.

Figure 4 shows the integral cross section for electron collisions with 1,2-butadiene molecules from 0.1 eV to 10 eV obtained in the SE and SEP approximations, along with the SEP cross section including the Born-closure, and the experimental TCS data of Szmytkowski et al. [9]. The SE cross section shows a peak at 4.3 eV and the inclusion of polarization effects moves the resonance to at around 2.4 eV. The present calculations are in good agreement with the TCS regarding the position of the resonance,

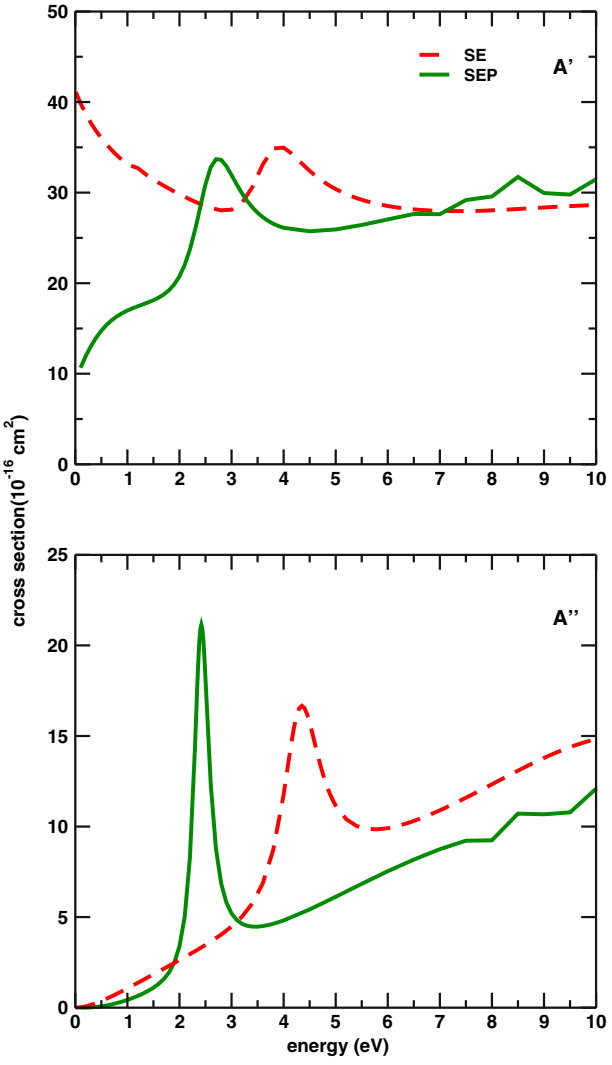

Fig. 5. Symmetry decomposition, in the C_s point group, of the integral elastic cross section for electron collisions with 1,2-butadiene in the SE and SEP approximations. See text for discussion.

which is also located at 2.4 eV in the experimental data. The inclusion of the permanent dipole effects on the cross section using the Born-closure procedure affects mainly the magnitude of the cross sections below 2 eV.

As for allene, pseudoresonances also appeared from 7 eV to 10 eV in SEP cross section. Full Single CI calculation at the present optimized geometry and with the scattering basis set provided the threshold for the first excited state at 3.58 eV. We have not found available results for comparison in the literature. The ionization channel does not contribute significantly to the scattering in the low-energy range, since the present calculated vertical ionization potential is 9.73 eV which compares well with the experimental value of 9.33 eV [26]. Again, the difference in magnitude between the present cross sections and the experimental TCS are due to the lack of electronic, vibrational and rotational excitation channels. Present calculations at SEP level with Born closure are tabulated in Table 4.

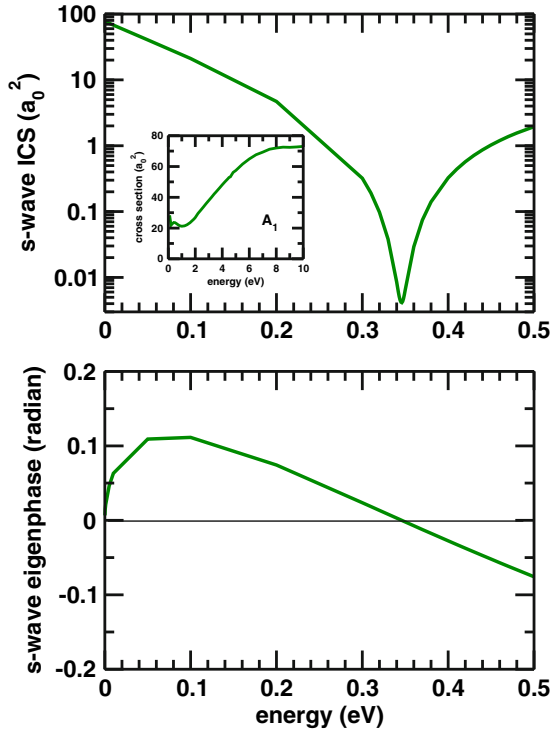

Fig. 6. The s-wave contribution to the integral cross section (ICS) obtained in the SEP approximation (upper panel) and the corresponding s-wave eigenphase (lower panel), for the allene. Inset figure: elastic cross section for the symmetry A_1 in the static-exchange plus polarization approximation. See text for discussion.

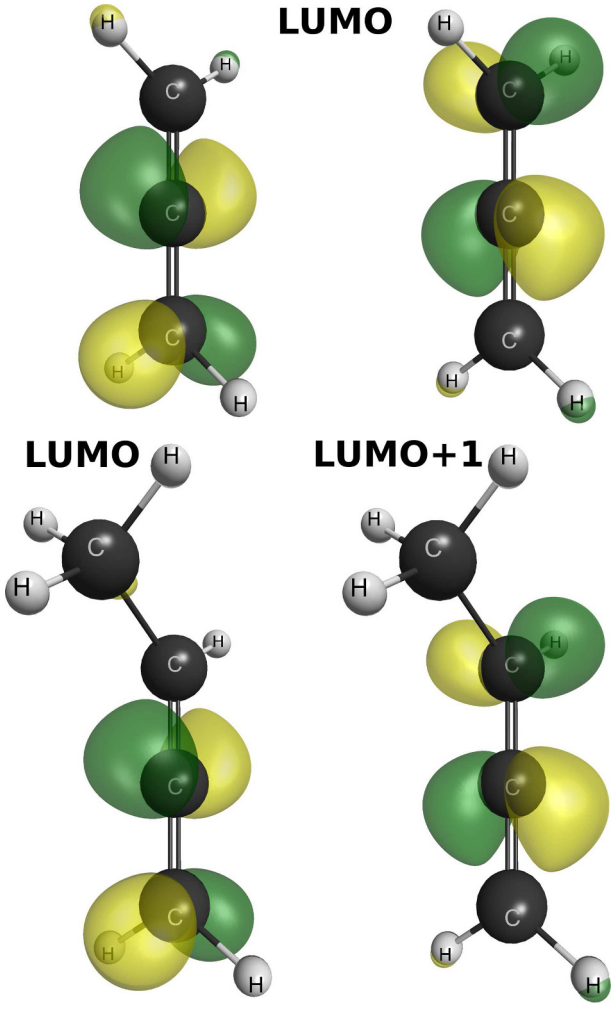

Fig. 7. Molecular orbitals: allene, b_1, b_2 LUMO (top); 1,2-butadiene, a' LUMO and a'' LUMO+1 (bottom). See text for discussion.

The symmetry decomposition of the integral cross section for 1,2-butadiene is shown in Figure 5, where the A' and A'' contributions are displayed in the SE and SEP approximations. There are, in the SE results, one structure at around 4 eV in the A' symmetry and another centered at 4.3 eV in the A''; the two structures overlap resulting in the resonance centered at 4.3 eV in the integral cross section. In the SEP calculations those structures moves to 2.6 eV and 2.4 eV, respectively, forming the peak centered at 2.4 eV. The fact that these two π^* resonances are located at slightly different energies reflects the symmetry breaking from D_{2d} (allene) to C_s (1,2-butadiene) as a consequence of the methylation.

As mentioned before, the A_1 symmetry of the allene molecule has no resonant structures. However, this symmetry presents a very interesting behavior in the low energy region, as can be seen in Figure 6 (upper panel). In order to unveil the origin of the shallow minimum appearing in the SEP integral cross section, we looked at the s-wave cross section (upper panel) and the corresponding eigenphase (lower panel) for energies up to 0.5 eV. These results show that the minimum is located at around 0.34 eV, and that the s-wave eigenphase changes sign, crossing zero, at this same energy. It is well known that for an attractive potential, the eigenphase is positive, and for a repulsive potential, it is negative. This change of sign in the eigenphase means that the potential changes from attractive to repulsive. In the SEP approximation, the net scattering potential is given by the static and polarization potentials, which are both attractive, and by the exchange potential, which is repulsive. The minimum observed in Figure 6 is the Ramsauer-Townsend minimum and occurs as a consequence of the cancellation between the above mentioned attractive and repulsive potentials [29,30].

Electronic structure calculations were employed to assign the resonant states to the correspondent molecular states. For both systems Hartree–Fock calculations with the 6-31G(1d) were performed with the computational package GAMESS [18] in order to obtain the plots of the unoccupied orbitals responsible for the resonances. For the allene molecule we have generated the plot for the degenerated pair of b_1 and b_2 symmetries corresponding to the LUMO, and for 1,2-butadiene molecule the a' and a'' orbitals corresponding to the LUMO and the LUMO+1, respectively, were generated. These plots are shown in Figure 7. The LUMO of allene is two-fold degenerated, being mainly located on the C=C bond with only a minor contribution near the H atoms and has an energy eigenvalue of 4.82 eV. The nodal planes of these π^* orbitals are in the plane formed by the C=C–H atoms, which

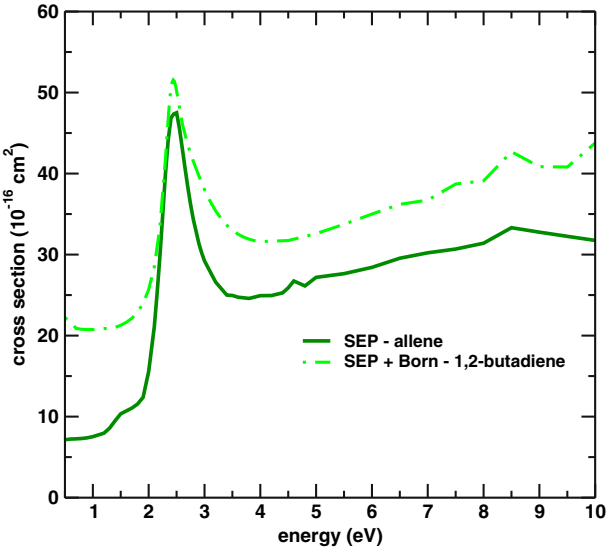

Fig. 8. Comparison between the integral elastic cross sections for electron collisions with allene and 1,2-butadiene in the static-exchange plus polarization approximation, including Born-closure in the 1,2-butadiene cross section. See text for discussion.

correspond to the symmetry planes of the molecule in the D_{2d} point group. For 1,2-butadiene molecule, we show the plots for the a' (LUMO) and the a'' (LUMO+1), whose energy eigenvalues are 4.91 eV and 5.03 eV, respectively. As for the allene molecule both are spatially distributed around the C=C bond, with minor contributions on the H and on the methyl group.

In Figure 8 we compare the integral elastic cross sections for both systems in the SEP approximation, with the Born-closure when necessary. The π^* resonance is located at the same energy of 2.4 eV. This is related to the similarity of the spacial location of the molecular orbitals assigned to these resonances. The same behaviour is verified with the TCS obtained by Szmytkowski and co-workers [2,9]. The resonances we have obtained are narrower and higher than the experimental data due to the neglect of nuclear vibration, since we used the fixed-nuclei approximation in our calculations [31]. The cross sections have a similar shape but they differ in magnitude, where the cross section of 1,2-butadiene is bigger than the allene cross section by a factor of about 1.2 for energies above 3 eV, in agreement with a previous methylation study carried out by Szmytkowski et al. [32]. Between 0.1 eV and 2 eV, this factor is higher, being approximately 3, showing the influence of the dipole moment in the low-energy scattering. The presence of a permanent electric dipole moment and the increase of the molecular size due to the extra methyl group are at the origin of this difference in magnitude.

A set of differential elastic cross sections at selected energies obtained in the SEP approximation for electron collisions with allene is shown in Figure 9 together with the experimental data measured by Nakano et al. [10], and the theoretical calculations of Barot et al. [14], and Sanchez et al. [12] in the SEP approximation. When comparing the present DCSs for allene with the experimental

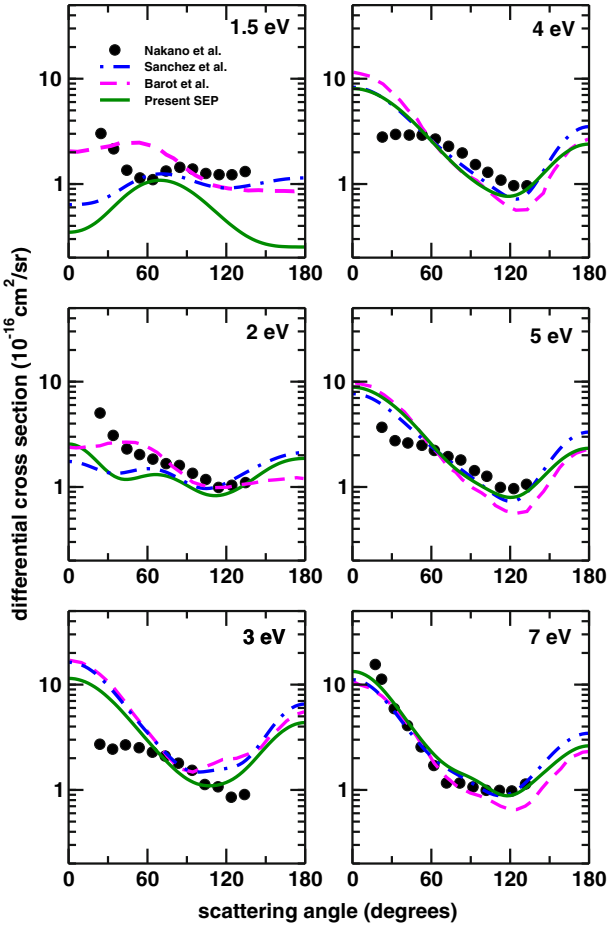

Fig. 9. Differential elastic cross sections for electron collisions with allene in the static-exchange plus polarization. The experimental elastic differential cross section obtained by Nakano et al. [10], and elastic differential cross sections calculated by Sanchez et al. [12], and by Barot et al. [14] are also shown.

data by Nakano we have found qualitative agreement between their magnitude for energies higher than 2 eV. At 1.5 eV a d-wave pattern with two minima at around 60° and 120° is visible in the experimental results, while in the present calculations these minima appear at 30° and 150°. From 2 eV to 5 eV this behavior remains but is less pronounced, with the scattering being more isotropic. At 7 eV the DCS at the low-angles increases significantly when compared with the previous energies. The d-wave pattern becomes again more visible. The present DCSs agree with the previous SMC calculations by Sanchez et al. [12] except at 1.5 eV (the tail of the π^* resonance). Although not shown in the article, Sanchez et al. [12] also reported a calculation with a large number of configurations, without significant changes in the cross section, except for an improvement in the position of the resonance. There is also a disagreement between the experimental results and the R-matrix calculations by Barot et al. [14], notoriously at 3 eV, probably due to the fact of the π^* resonance being centered at 2.9 eV in their TCS.

In Figure 10 we compare the DCSs for allene in the SEP approximation with the DCSs for 1,2-butadiene in

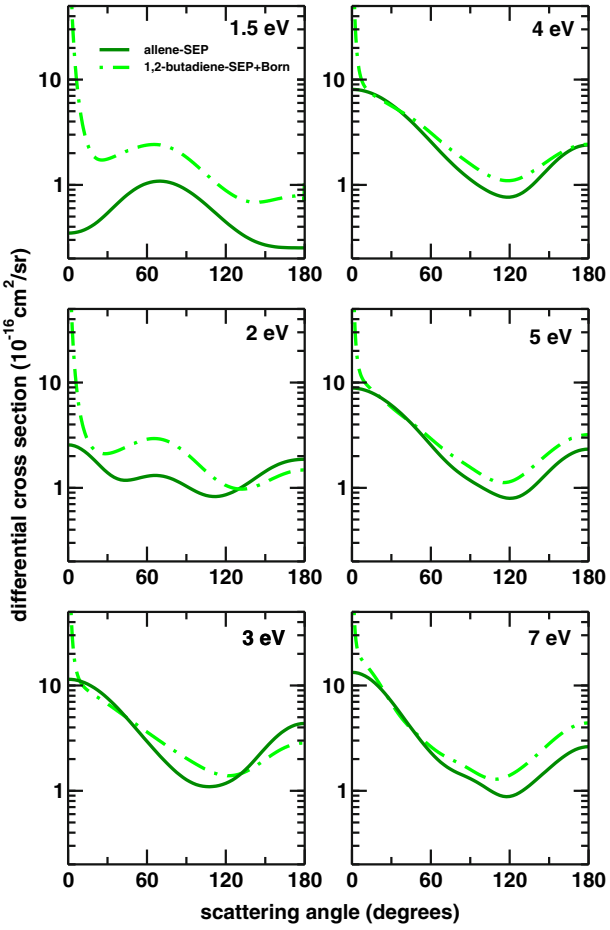

Fig. 10. Comparison between the differential elastic cross sections for electron collisions with allene and 1,2-butadiene in the static-exchange plus polarization approximation, including the Born-closure procedure in the 1,2-butadiene cross section.

the same approximation. The dipole effects included by the Born-closure in the 1,2-butadiene increase the DCSs for angles lower than 15°. A *d*-wave pattern is noticeable for 1.5 eV and 2 eV but, for 3–7 eV the forward scattering increases and only the minimum centered at 120° remains. Comparing the present calculations for both systems, we can notice the dipole signature at low-angles in the 1,2-butadiene DCSs. In general the DCSs of 1,2-butadiene are bigger than the DCSs of allene for lower energies, and become closer as the energy increases. These aspects of the DCSs can be viewed as a consequence of the methylation, since the CH_3 group in 1,2-butadiene is responsible for its permanent dipole moment. There is also an increase in the geometrical size of 1,2-butadiene in comparison with allene, which is reflected in the magnitude of the scattering cross sections.

4 Summary

In this paper we have performed calculations for low-energy electron scattering by allene and 1,2-butadiene molecules. Electronic structure calculations were used to aid in the interpretation of the collision results. For both molecular targets we have found a π^* shape resonance centered at 2.4 eV and assigned them to the molecular orbitals wich are spatially located surrounding the C=C bonds. A Ramsauer-Townsend minimum was found at 0.34 eV in the integral cross section of allene. As the result of the methylation effect on the cross section we have pointed the permanent dipole moment, the increase in the magnitude of the integral cross section and the break of symmetry in the resonant symmetries for 1,2-butadiene in comparison to allene.

G.M.M., T.C.F., and M.H.F.B. acknowledge support from Brazilian agencies Conselho Nacional de Desenvolvimento Científico e Tecnológico (CNPq), and Coordenação de Aperfeiçoamento Pessoal de Nível Superior (CAPES). The authors acknowledge computational support from Professor Carlos M. de Carvalho at LFTC-DFis-UFPR and at LCPAD-UFPR, and from CENAPAD-SP.

Author contribution statement

G.M.M. and T.C.F. performed electron scattering cross section calculations using the SMCPP method. All authors contributed to the analyses and discussion of the results and also in paper writing and proof reading.

References

1. M.C.A. Lopes, D.G.M. Silva, M.H.F. Bettega, D.F. da Costa, M.A.P. Lima, M.A. Khakoo, C. Winstead, V. McKoy, J. Phys.: Conf. Ser. **388**, 012014 (2012)
2. C. Szmytkowski, S. Kwitnewski, J. Phys. B: At. Mol. Opt. Phys. **35**, 3781 (2002)
3. D. Field, Europhys. News **36**, 51 (2005)
4. M.A. Lieberman, A.J. Lichtenberg, *Principles of Plasma Discharges and Materials Processing* (John Wiley & Sons, New York, 1994)
5. W.N.G. Hitchon, *Plasma Processes for Semiconductor Fabrication* (Cambridge University Press, Cambridge, 1999)
6. L.G. Christophorou, J.K. Olthoff, *Fundamental Electron Interactions with Plasma Processing Gases* (Kluwer, New York, 2004)
7. J. Collin, F.P. Lossing, J. Am. Chem. Soc. **79**, 5848 (1957)
8. L.J. Schaad, L.A. Burnelle, K.P. Dressler, Theor. Chem. Acc. **15**, 91 (1969)
9. C. Szmytkowski, P. Możejko, M. Zawadzki, E.S. Ptasińska-Denga, J. Phys. B: At. Mol. Opt. Phys. **48**, 025201 (2015)
10. Y. Nakano, M. Hoshino, M. Kitajima, H. Tanaka, M. Kimura, Phys. Rev. A **66**, 032714 (2002)
11. C. Makochekanwa, H. Kawate, O. Sueoka, M. Kimura, M. Kita-Jima, M. Hoshino, H. Tanaka, Chem. Phys. Lett. **368**, 82 (2003)
12. S.d'A. Sanchez, A.R. Lopes, M.H.F. Bettega, M.A.P. Lima, L.G. Ferreira, Phys. Rev. A **71**, 062702 (2005)
13. L. Chiari, A. Zecca, F. Blanco, G. García, M.J. Brunger, J. Chem. Phys. **144**, 084301 (2016)
14. A. Barot, D. Gupta, M. Vinodkumar, B. Antony, Phys. Rev. A **87**, 062701 (2013)

15. K. Takatsuka, V. McKoy, Phys. Rev. A **24**, 2473 (1981)
16. K. Takatsuka, V. McKoy, Phys. Rev. A **30**, 1734 (1984)
17. R.F. da Costa, M.T. do N. Varella, M.H.F. Bettega, M.A.P. Lima, Eur. Phys. J. D **69**, 159 (2015)
18. M.W. Schmidt, K.K. Baldridge, J.A. Boatz, S.T. Elbert, M.S. Gordon, J.H. Jensen, S. Koseki, N. Matsunaga, K.A. Nguyen, S.J. Su, T.L. Windus, M. Dupuis, J.A. Montgomery, J. Comput. Chem. **14**, 1347 (1993)
19. G. Herzberg, *Electronic Spectra and Electronic Structure of Polyatomic Molecules* (Van Nostrand, New York, 1966)
20. K. Kuchitsu, *Landolt-Bornstein: Group II: Atomic and Molecular Physics Volume 21: Structure Data of Free Polyatomic Molecules* (Springer-Verlag, Berlin, 1992)
21. B.M. Bode, M.S. Gordon, J. Mol. Graph. Model. **16**, 133 (1998)
22. G.B. Bachelet, D.R. Hamann, M. Schlüter, Phys. Rev. B **26**, 4199 (1982)
23. M.H.F. Bettega, A.P.P. Natalense, M.A.P. Lima, L.G. Ferreira, Int. J. Quantum Chem. **60**, 821 (1996)
24. W.J. Hunt, W.A. Goddard III, Chem. Phys. Lett. **3**, 414 (1969)
25. C. Winstead, V. McKoy, Phys. Rev. A **57**, 3589 (1998)
26. NIST Computational Chemistry Comparison and Benchmark Database NIST Standard Reference Database Number 101 Release 20, August 2019, edited by R.D. Johnson, III, http://cccbdb.nist.gov/
27. E. M. de Oliveira, R.F. da Costa, S.d'A. Sanchez, A.P.P. Natalense, M.H.F. Bettega, M.A.P. Lima, M.T. do N. Varella, Phys. Chem. Chem. Phys. **15**, 1682 (2013)
28. M.T. do N. Varella, M.H.F. Bettega, M.A.P. Lima, L.G. Ferreira, J. Chem. Phys. **111**, 6396 (1999)
29. M.A.P. Lima, K. Watari, V. McKoy, Phys. Rev. A **39**, 4312 (1989)
30. B.M. Nestmann, K. Pfingst, S.D. Peyerimhoff, J. Phys. B **27**, 2297 (1994)
31. T.N. Rescigno, D.A. Byrum, W.A. Isaacs, C.W. McCurdy, Phys. Rev. A **60**, 2186 (1999)
32. C. Szmytkowski, S. Stefanowska, M. Zawadzki, E. Ptasińska-Denga, P. Możejko, Phys. Rev. A **94**, 042706 (2016)